Hindawi
Wireless Communications and Mobile Computing
Volume 2021, Article ID 6673807, 12 pages
https://doi.org/10.1155/2021/6673807

WILEY | Hindawi

Research Article

Impact of IQ Imbalance on RIS-Assisted SISO Communication Systems

Asma Bouhlel[1] **and Anis Sakly**[2]

[1]*Laboratory of Electronic and Micro-Electronic, Faculty of Sciences Monastir, University of Monastir, Tunisia*
[2]*Laboratory of Industrial Systems Study and Renewable Energy, National Engineering School of Monastir, Tunisia*

Correspondence should be addressed to Asma Bouhlel; bouhlel_asmaa@yahoo.fr

Received 16 November 2020; Revised 2 July 2021; Accepted 23 July 2021; Published 15 August 2021

Academic Editor: Mumtaz Shahid

Reconfigurable intelligent surface (RIS) for wireless networks has emerged as a promising future transmission technique to create smart radio environments that improve the system performance by turning the wireless channel into an adjustable system block. However, transceivers come with various hardware impairments, such as phase noise and in-phase/quadrature-phase imbalance (IQI). Hence, for robust configuration of RIS-based communication under practical conditions, assuming the identical performance analysis when subject to IQI, will lead to inaccurate analysis. In this paper, the implementation of this novel transmission technique is thoroughly investigated under intensive realistic circumstances. For this purpose, based on the maximum likelihood (ML) detector, a novel analytical expression of average pairwise error probability under IQI is proposed and compared to the standard ML detector. Further, the proposed analytical approaches are confirmed by numerical simulations.

1. Introduction

Many attempts have been done in recent years to deliver new deployment models with high speeds, superior reliability, and negligible latency to meet the requirements of 5G standards. To achieve these goals, several transmission techniques have been used such as millimeter wave (mmWave), orthogonal frequency division multiplexing (OFDM), and massive multiple input multiple output (MIMO) [1]. Although the successful launch of the first 5G service, the introduced technologies suffer from high energy consumption and uncontrolled propagation environments effects. Therefore, for the sixth-generation (6G) mobile communication systems with very-high frequency bands and more power efficiency, researchers are already exploring new methods [2] such as reconfigurable intelligent surface (RIS) [3]. RIS, also known as large intelligent surface (LIS) [4], has attracted a significant amount of attention from researchers as a promising future transmission technique to create a smart propagation environment [5, 6]. Conventionally, only the source and the destination are controlled with coding, encoding, and many processing operations to enhance the quality of the signal. By putting a RIS between the transmitter (Tx) and the receiver (Rx), an additional propagation path appears. Thus, the created channel behavior can be software-controlled in order to achieve a smart programmable wireless environment that provides more freedom degrees and boost the performance [6].

The announced technique has been compared with the massive MIMO [7], amplify-and-forward (AF) relaying [8], backscatter communication [9], mmWave communication [10], and network densification [11]. Although it is similar to other existing technologies, the RIS is based on a large number of thin passive reflectors without buffering and processing any incoming signals [4]. These reflectors are designed based on two-dimensional meta-surfaces [12, 13]. In addition, RIS is equipped with a programmable microcontroller that modifies the phase of the incident electromagnetic waves in a way that can enhance the signal quality at the Rx and improve the network coverage. Hence, RIS improves the quality of the received signal by simply reflecting and adjusting the incident signal phase shifts favorably

with low cost and low energy consumption [3]. The novel proposed concept presents important theoretical and electromagnetic design challenges [14, 15].

However, the use of RIS poses several new challenges for the transceiver design, and it is paramount to analyze the system performance under practical conditions [16]. Accordingly, RIS-aided communication performance can be significantly degraded by different types of realistic imperfections, including noise signal, imperfect channel state information (CSI), and transceiver hardware impairments. The effect of the hardware impairments general model on the achievable rate of RIS has been studied in [17]. In [18, 19], an asymptotic analysis of the uplink data rate in a RIS-based communication system affected by channel estimation errors and interference was investigated. The design and the implementation of RIS were also detailed in [20].

To the best of the authors' knowledge, RIS under in-phase and quadrature imbalance (IQI) has not been highlighted yet. However, for robust configuration, modeling the transceiver radio frequency (RF) front-end hardware as perfect will lead to inaccurate analysis [21]. Indeed both in-phase (I) and quadrature (Q) modulator and demodulator at the Tx and Rx may introduce phase and/or amplitude mismatch [22]. Additional harmful effects could degrade the system performance such as crosstalk and frequency interference [23–25]. Hence, taking into account IQI effects is a crucial factor for RIS effective design policies.

Motivated by the aforementioned limitations of the existing literature, this paper explores the design of an optimal Rx detector which is compared to the performance of the classical ML in the presence of IQI. Accordingly, novel error probability analytical expressions are derived and proved with simulation results.

2. System Model and Signal Detection

2.1. System Model. In this section, we have adapted a general RIS-assisted single-input single output (SISO) wireless communication system as presented in Figure 1. The direct signal path between the source and the destination is ignored in the rest of the paper [4], and the RIS is deployed to relay the scattered signal. Indeed, this assumption holds in the case of unfavorable propagation conditions that might be caused by an obstacle or a long distance, for example, [26–28].

First, the information is conveyed from the source to the RIS. Then, the RIS software controls the amplitude and the phase of the received signal to combat the propagation environment's harmful effects and reflect it to the destination.

Although RIS is based on small passive elements and does not need any signal processing power, the font-ends of both Tx and Rx could be affected by the IQI which limits the system performance. Actually in practical conditions, due to the local oscillator (LO), filters, analog components, and up-and-down-conversion steps at Tx and Rx sides, the generated signals present a mismatch between the I and Q parts [29]. Accordingly, the Tx and Rx sides IQI parameters are introduced, respectively, using (G_1, G_2) and (K_1, K_2) which can be expressed while based on the complex LO signals [24, 30] as

$$G_1 = \frac{1}{2}\left(1 + \xi_t e^{j\varphi_t}\right), G_2 = \frac{1}{2}\left(1 - \xi_t e^{-j\varphi_t}\right), \tag{1}$$

$$K_1 = \frac{1}{2}\left(1 + \xi_r e^{-j\varphi_r}\right), K_2 = \frac{1}{2}\left(1 - \xi_r e^{j\varphi_r}\right), \tag{2}$$

where (ξ_t, φ_t) and (ξ_r, φ_r) denote, respectively, Tx and Rx amplitude and phase imbalances. In the ideal case, where the IQ branch is perfectly matching these parameters that are reduced to $\xi_t = \xi_r = 1$ and $\varphi_t = \varphi_r = 0°$. Consequently, we have $G_1 = K_1 = 1$ and $G_2 = K_2 = 0$. The up-converted signal modulated over M-ary mapper at the source affected by IQI can be written as

$$x^{IQ} = G_1 x + G_2 x^*, \tag{3}$$

where $()^*$ denotes the complex conjugate.

Using RIS with N reflectors, the signal is firstly transmitted from the source antenna to the RIS then it is conveyed from the RIS to the destination through, respectively, the flat fading channels h_k and g_k for the k^{th} reflecting meta-surface $(k = 1, 2, \cdots, N)$. Note that h_k, g_k follow zero-mean complex Gaussian distribution with unit variance.

In such case, an intelligent RIS software is deployed to adjust the reflection phases based on the channel phases in order to maximize the received SNR. Hence, the adjustable signal received at the destination is given as

$$y = \sqrt{P}\left[\sum_{k=1}^{N} h_k e^{j\varphi_k} g_k\right] x^{IQ} + n, \tag{4}$$

where φ_k characterizes the adapted phase for the k^{th} RIS reflector, P is the average of the transmitted power symbol, and n is a complex additive white Gaussian noise (AWGN) with zero mean and N_0 variance. Using (3), the received signal becomes

$$y = \sqrt{P}\left[\sum_{k=1}^{N} h_k e^{j\varphi_k} g_k\right] [G_1 x + G_2 x^*] + n. \tag{5}$$

Taking into account the Rx IQI and the adjusted phases, the resulting signal at the destination can be expressed as

$$\begin{aligned} y^{IQ} &= K_1 y + K_2 y^* \\ &= \underbrace{\sqrt{P}\left[K_1 G_1 \sum_{k=1}^{N} h_k e^{j\varphi_k} g_k + K_2 G_2^* \sum_{k=1}^{N} h_k^* e^{-j\varphi_k} g_k^*\right] x}_{S} \\ &\quad + \underbrace{\sqrt{P}\left[K_1 G_2 \sum_{k=1}^{N} h_k e^{j\varphi_k} g_k + K_2 G_1^* \sum_{k=1}^{N} h_k^* e^{-j\varphi_k} g_k^*\right] x^*}_{I} \\ &\quad + K_1 n + K_2 n^* = \left(\sqrt{P} S x + \sqrt{P} I x^*\right) + \eta = \sqrt{P}\chi + \eta, \end{aligned} \tag{6}$$

where $\chi = Sx + Ix^*$ and $\eta = K_1 n + K_2 n^*$.

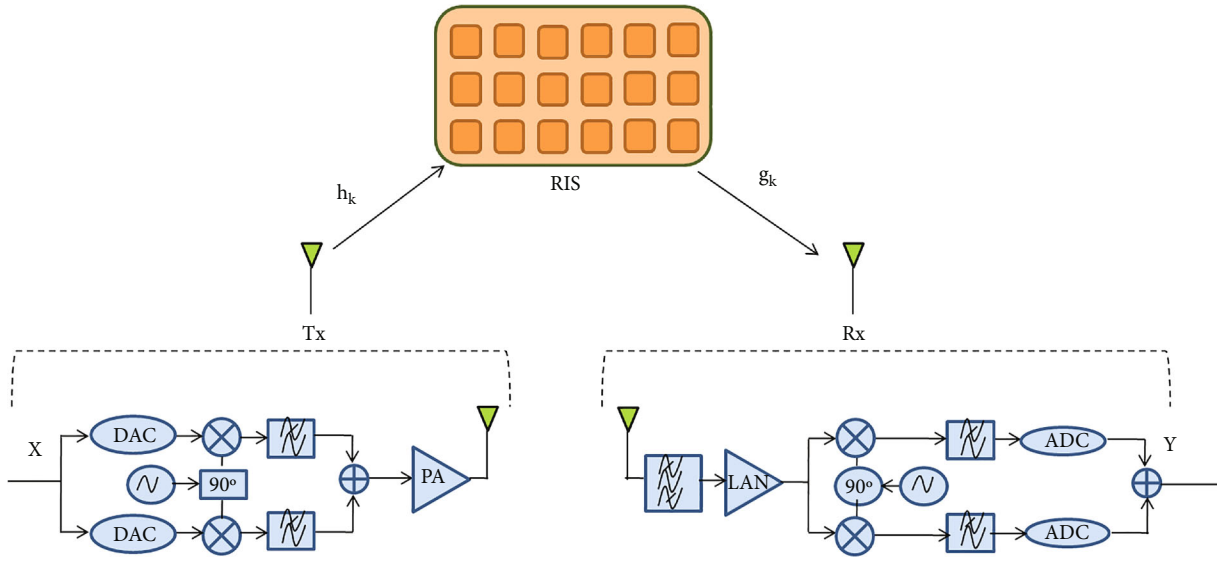

Figure 1: RIS under IQI system model.

Note that due to Tx and Rx IQI, the baseband signal x is interfered by its complex conjugate x^*. Hence, Ix^* represents the self-interferences.

Analogous to [4], with the assistance of a software communication, the following derived expressions are analyzed based on the knowledge of the channel at the RIS in function of amplitudes and phases as $h_k = \varepsilon_k e^{-j\theta_k}$, $g_k = \beta_k e^{-j\psi_k}$. In such case, the RIS adjusts the phases in order to maximize the signal-to-noise ratio (SNR) such as $\varphi_k = \theta_k + \psi_k$.

Moreover, the noise can be expressed as $\eta = n^I + j(K_c n^I + K_d n^Q)$ where n^I and n^Q note, respectively, the real and imaginary parts of n, $K_c = K_1^Q + K_2^Q$, and $K_d = K_1^I - K_2^I$ [23].

Accordingly, stating that $\eta = \eta^I + j\eta^Q$ where η^I and η^Q note, respectively, the real and imaginary parts of η, it is worth noting that η is an improper Gaussian noise with unequal real and imaginary parts variances such as

$$\sigma_{\eta^I}^2 = \frac{\sigma_n^2}{2} = \frac{N_0}{2}, \tag{7}$$

$$\sigma_{\eta^Q}^2 = \left(K_c^2 + K_d^2\right)\frac{\sigma_n^2}{2} = \frac{N_0}{2}\xi_r^2. \tag{8}$$

Further, the correlation factor between the noise components is $\rho = \text{cov}\,(\eta^I, \eta^Q)/\sigma_{\eta^I}\sigma_{\eta^Q} = K_c(\sigma_n^2/2)/\xi_r\sigma_n^2/2 = -\sin(\varphi_r)$ [25]. It is important to emphasize the IQI effects in changing the behavior of the noise from proper to improper. Thus, the received signal has correlated IQ components. Considering the presence of improper noise is a critical factor in analyzing the RIS performance.

The received signal expression in (6) can be analyzed under several scenarios taking into account the possible values of IQ parameters:

(1) *Perfect IQ Matching*. In this scenario, Tx and Rx sides are assumed to be perfect and IQI parameters are defined as $\boldsymbol{G_1} = \boldsymbol{K_1} = \mathbf{1}, \boldsymbol{G_2} = \boldsymbol{K_2} = \mathbf{0}$. The received signal in (6) can be expressed as the following well known expressed used for all previous studies:

$$y = \sqrt{P}\left[\sum_{k=1}^{N}\varepsilon_k\beta_k\right]x + n. \tag{9}$$

(2) *Tx Impaired by IQI*. Taking into account the destructive effects of only the Tx side with perfect IQI parameters on the destination, i.e., $\boldsymbol{K_1} = \mathbf{1}$ and $\boldsymbol{K_2} = \mathbf{0}$, the resulting signal is given as

$$y_{Tx}^{IQ} = \sqrt{P}\left[\sum_{k=1}^{N}\varepsilon_k\beta_k\right][G_1 x + G_2 x^*] + n. \tag{10}$$

(3) *Rx Impaired by IQI*. Considering ideal Tx IQI parameters and stating that $\boldsymbol{G1} = \mathbf{1}, \boldsymbol{G2} = \mathbf{0}$, (6) can be rewritten as

$$y_{Rx}^{IQ} = \sqrt{P}\left[\sum_{k=1}^{N}\varepsilon_k\beta_k\right][K_1 x + K_2 x^*] + K_1 n + K_2 n^*. \tag{11}$$

It can be observed from the above expressions that Tx impaired with IQI causes self-interference from the conjugate of the transmitted signal. On the other side, Rx suffering from IQI affects both the signal and the noise.

As previously mentioned, with the presence of IQI, a new derived received signal expression is required which shows the presence of self-interference and new noise behavior.

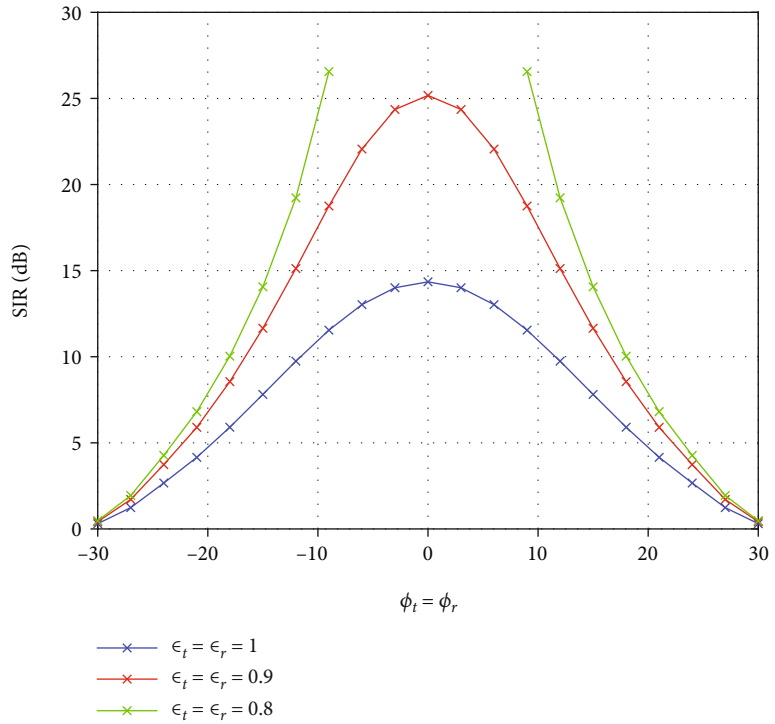

Figure 2: SIR values variation of RIS under IQI in function of phases with fixed gains $\varepsilon_t = \varepsilon_r = [0.8,0.9,1]$.

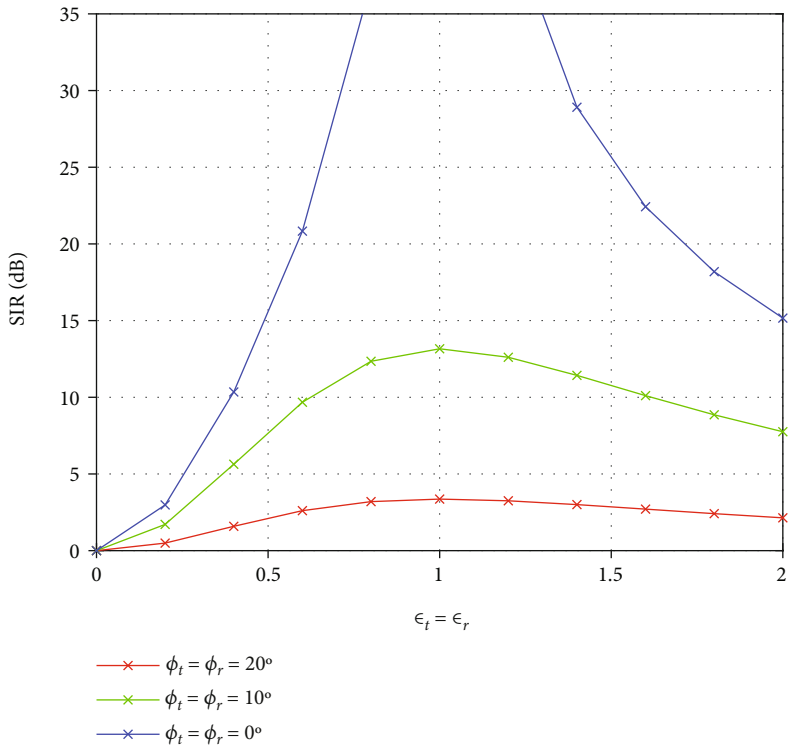

Figure 3: SIR values variation of RIS under IQI in function of gains with fixed phases $\phi_t = \phi_r = [0^\circ, 10^\circ, 20^\circ]$.

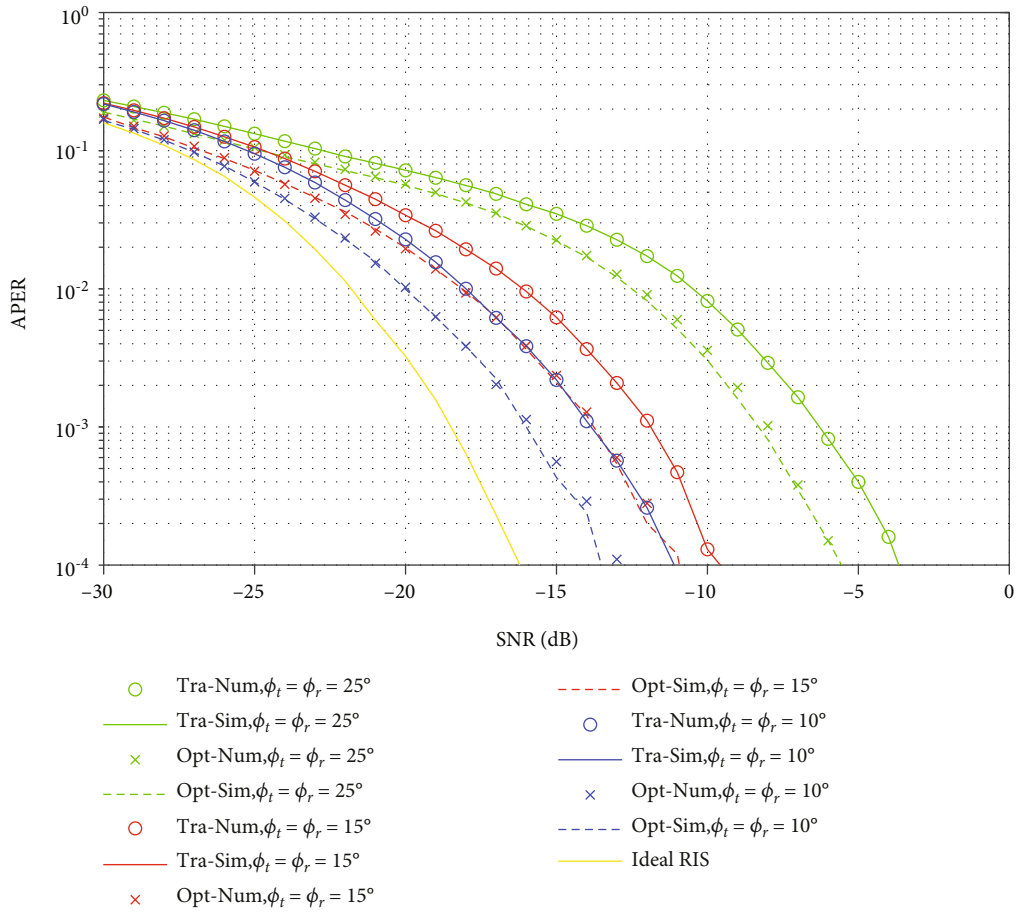

FIGURE 4: RIS APEP of optimal and traditional ML detector under IQI in function of phases with fixed gains $\varepsilon_t = \varepsilon_r = 3$dB using $N = 32$ and 4-QAM.

Hence, for an effective performance study of RIS-based communication systems, a novel design of optimal ML detector that incorporates the IQI effects is obligatory.

2.2. Signal-to-Interference Ratio (SIR). The average SIR is calculated as follows to illustrate the harmful effects of the caused self-interference

$$\mathrm{SIR} = \frac{\mathbb{E}\{|S|^2\}}{\mathbb{E}\{|I|^2\}}. \tag{12}$$

Note that the image rejection ratio IRR which denotes the measure of image frequency band attenuation can be defined for Tx and Rx sides, respectively, as $\mathrm{IRR}_{Tx} = |G_1|^2/|G_2|^2$ and $\mathrm{IRR}_{Rx} = |K_1|^2/|K_2|^2$ [31]. IRR has a typical value in the range of 20-40 dB for practical analog RF front-end electronics [32]. Based on (2), the following relation can be defined $K_1 = 1 - K_2^*$. It can be depicted that for high IRR_{Rx} values $K_1 \longrightarrow 1$ and, $K_1 K_2^* = K_1 - K_1^2 \longrightarrow 0$ [33]. Supposing $\gamma_k = \varepsilon_k \beta_k$, an approximate widely used in the literature [31–34] is obtained by assuming

$$\begin{aligned}
&\mathbb{E}\left\{\left[\sum_{k=1}^{N}\gamma_k\right]^2\right\}\left(|K_1|^2|G_1|^2 + |K_2|^2|G_2|^2\right) \\
&>>\mathbb{E}\left\{2\Re\left(K_1 G_1 K_2^* G_2\left[\sum_{k=1}^{N}\gamma_k\right]^2\right)\right\}\mathbb{E}\left\{\left(\sum_{k=1}^{N}\gamma_k\right)^2\right\} \\
&\quad\times\left(|K_1|^2|G_2|^2 + |K_2|^2|G_1|^2\right) \\
&>>\mathbb{E}\left\{2\Re(K_1 G_2 K_2^* G_1\left[\sum_{k=1}^{N}\gamma_k\right]^2\right\}.
\end{aligned} \tag{13}$$

Hence, the averaged SIR can be tightly approximated as

$$\mathrm{SIR} \simeq \frac{|K_1|^2|G_1|^2 + |K_2|^2|G_2|^2}{|K_1|^2|G_2|^2 + |K_2|^2|G_1|^2}. \tag{14}$$

It is obviously seen that even small values of IQI degrade the system performance. Further, the SIR expression is independent of N. Hence, increasing the reflector number cannot mitigate the interference caused by the IQI. In the ideal case of perfect IQ matching SIR = ∞.

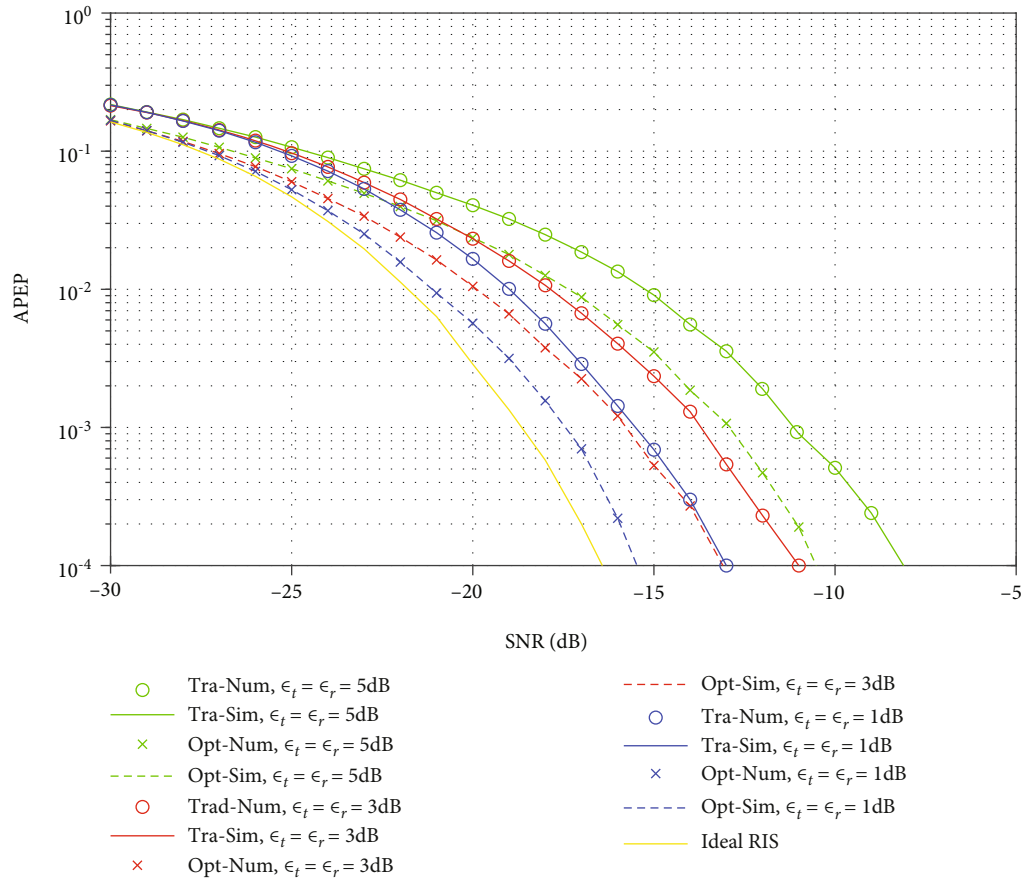

FIGURE 5: RIS APEP of optimal and traditional ML detector under IQI in function of gains with fixed phases $\phi_t = \phi_r = 10^\circ$ using $N = 32$ and 4-QAM.

2.3. Signal Detection

2.3.1. Optimal ML Detector. In the attempt to cover the presence of an improper Gaussian noise, an optimal ML detector is designed based on the received signal expression in (6). Hence, the bivariate Gaussian random variable (RV) distribution of the real, y_{IQ}^I, and imaginary, y_{IQ}^Q, correlated components of the received signal vector y is described as follows:

$$f_{y_{IQ}^I, y_{IQ}^Q}\left(y_{IQ}^I, y_{IQ}^Q \mid x\right) = \left(\frac{1}{2\pi\sigma_{\eta^I}\sigma_{\eta^Q}\sqrt{1-\rho^2}}\right) \exp\left(-\frac{1}{2(1-\rho^2)}\left[\frac{\left\|y_{IQ}^I - \sqrt{P}\chi^I\right\|^2}{\sigma_{\eta^I}^2} + \frac{\left\|y_{IQ}^Q - \sqrt{P}\chi^Q\right\|^2}{\sigma_{\eta^Q}^2} - \frac{2\rho\left(y_{IQ}^I - \sqrt{P}\chi^I\right)\left(y_{IQ}^Q - \sqrt{P}\chi^Q\right)}{\sigma_{\eta^I}\sigma_{\eta^Q}}\right]\right), \tag{15}$$

where χ^I and χ^Q represent, respectively, $\Re\{\chi\}$ and $\Im\{\chi\}$ components.

Regarding that the transmitted symbols are assumed equally distributed, the optimal ML detector is given by maximizing the argument of the conditional joint probability density function (PDF) defined in (15) which is equivalent to the following expression:

$$\{\widehat{x}\}_{\mathrm{ML}_{op}} = \arg\min_x \left\{\frac{\left\|y_{IQ}^I - \sqrt{P}\chi^I\right\|^2}{\sigma_{\eta^I}^2} + \frac{\left\|y_{IQ}^Q - \sqrt{P}\chi^Q\right\|^2}{\sigma_{\eta^Q}^2} - \frac{2\rho\left(y_{IQ}^I - \sqrt{P}\chi^I\right)\left(y_{IQ}^Q - \sqrt{P}\chi^Q\right)}{\sigma_{\eta^I}\sigma_{\eta^Q}}\right\}. \tag{16}$$

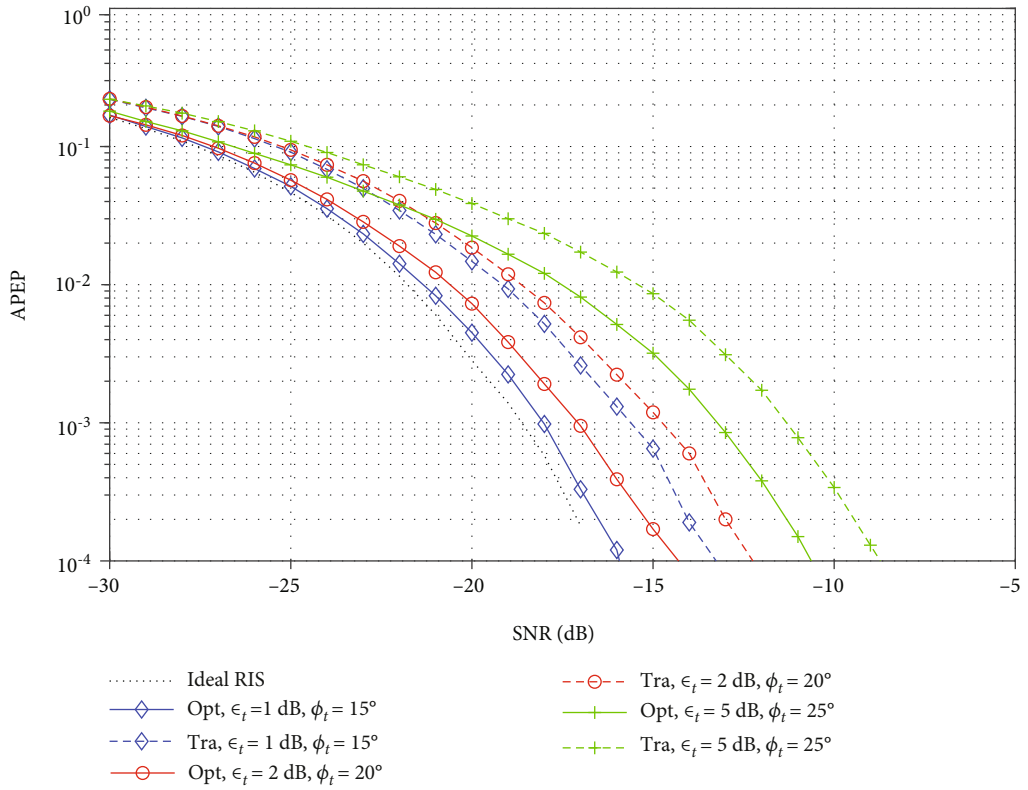

Figure 6: RIS APEP of optimal and traditional ML detector in the presence of Tx IQI with $N = 32$ using 4-QAM.

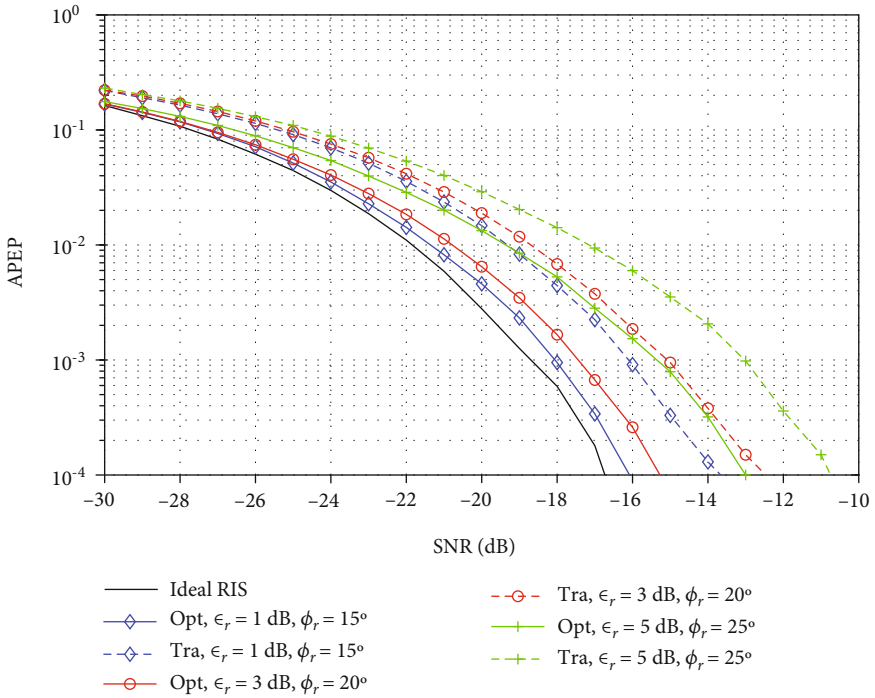

Figure 7: RIS APEP of optimal and traditional ML detector in the presence of Rx IQI with $N = 32$ using 4-QAM.

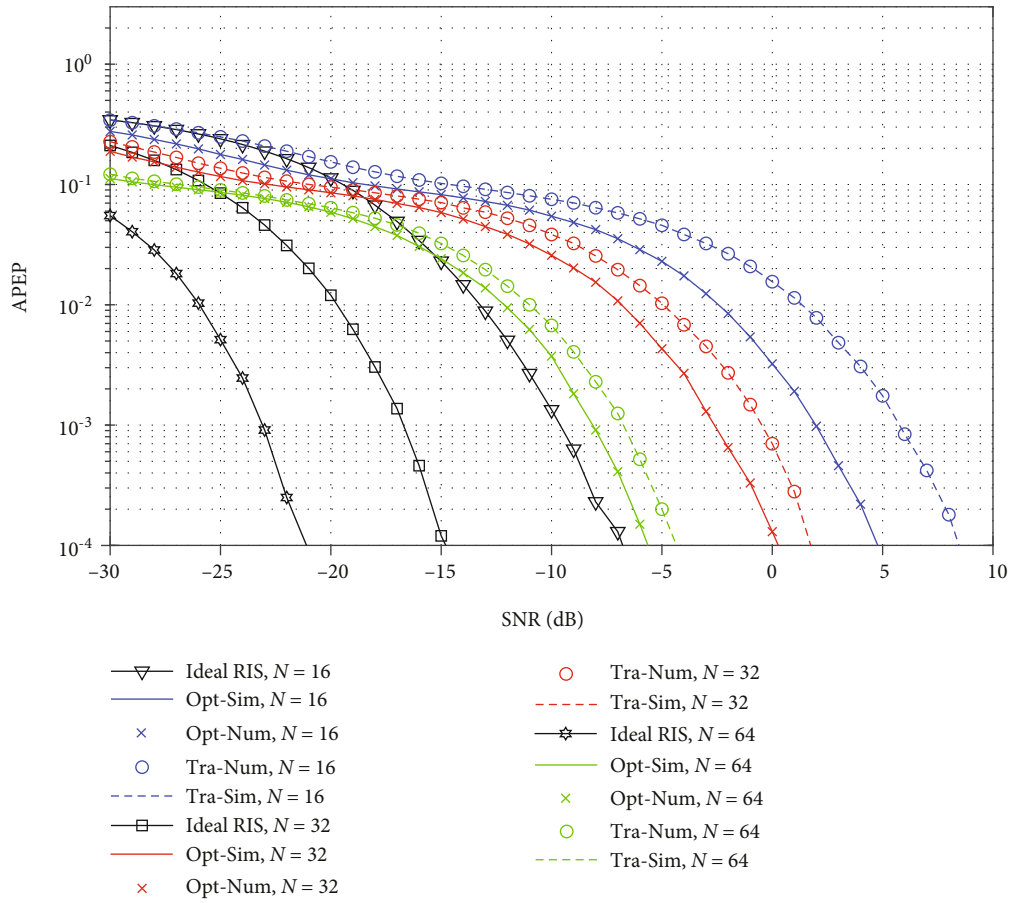

FIGURE 8: RIS APEP of optimal and traditional ML detector in the presence of joint Tx and Rx IQI with $\varepsilon_t = \varepsilon_r = 5\text{dB}$, $\phi_t = \phi_r = 20°$, and $N = [16,32,64]$ using 4-QAM.

2.3.2. Traditional ML Detector. The traditional ML detector is the classical ML detector used in the previous performance analysis of RIS in which the presence of IQI in the received signal expression is neglected. Indeed, it is simply expressed as the following well-known expression used for all previous studies of RIS performance:

$$\{\hat{x}\}_{\mathrm{ML}_{tra}} = \arg \min_{x} \left\{ \left\| y^{IQ} - \sqrt{P}\chi \right\|^2 \right\}. \tag{17}$$

3. Performance Analysis

3.1. Conditional Error Probability

3.1.1. Optimal ML Detector. Assuming χ is transmitted, the pairwise error probability (PEP) of deciding in favor of $\tilde{\chi}$ is given from the optimal ML detector expression in (16) as

$$\begin{aligned}\mathrm{PEP}_{\mathrm{opt}} &= \mathrm{P}_r \left\{ \frac{\left\| y_{IQ}^{I} - \sqrt{P}\chi^{I} \right\|^2}{\sigma_{\eta^I}^2} + \frac{\left\| y_{IQ}^{Q} - \sqrt{P}\chi^{Q} \right\|^2}{\sigma_{\eta^Q}^2} - \frac{2\rho\left(y_{IQ}^{I} - \sqrt{P}\chi^{I}\right)\left(y_{IQ}^{Q} - \sqrt{P}\chi^{Q}\right)}{\sigma_{\eta^I}\sigma_{\eta^Q}} > \frac{\left\| y_{IQ}^{I} - \sqrt{P}\tilde{\chi}^{I} \right\|^2}{\sigma_{\eta^I}^2} + \frac{\left\| y_{IQ}^{Q} - \sqrt{P}\tilde{\chi}^{Q} \right\|^2}{\sigma_{\eta^I}^2} - \frac{2\rho\left(y_{IQ}^{I} - \sqrt{P}\tilde{\chi}^{I}\right)\left(y_{IQ}^{Q} - \sqrt{P}\tilde{\chi}^{Q}\right)}{\sigma_{\eta^I}\sigma_{\eta^Q}} \right\} \\ &= \Pr\{\beta > 0\},\end{aligned} \tag{18}$$

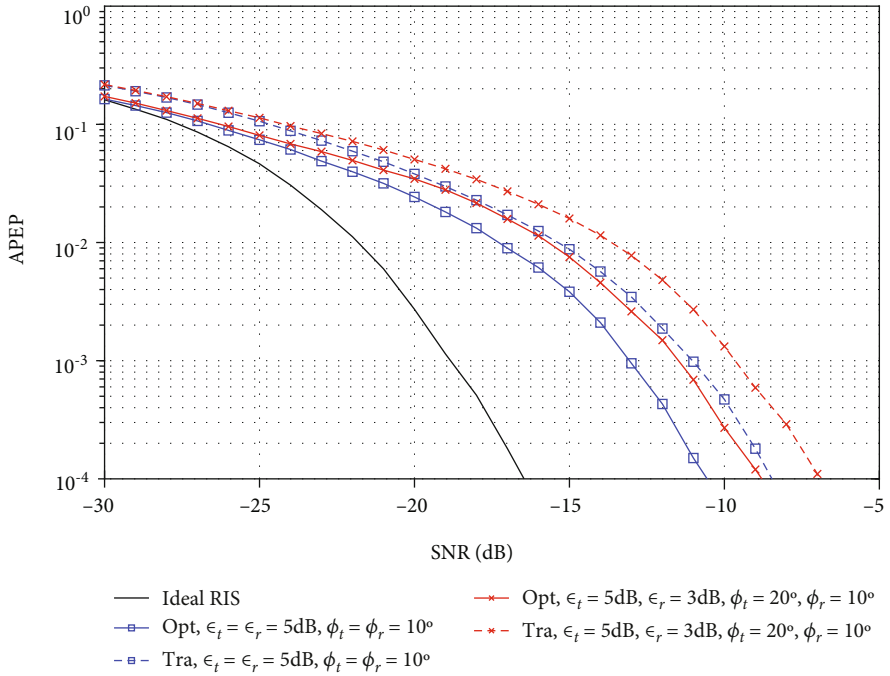

FIGURE 9: RIS APEP of optimal and traditional ML detector in the presence of joint Tx and Rx IQI with $\varepsilon_t = \varepsilon_r = 5$dB, $\phi_t = \phi_r = 10^\circ$ and $\varepsilon_t = 5$dB, $\varepsilon_r = 3$dB, $\phi_t = 20^\circ$, $\phi_r = 10^\circ$, and $N = 32$ using 4-QAM.

where $\tilde{\chi} = S\tilde{x} + I\tilde{x}^*$ and β is obtained after simple mathematical operations as

$$\begin{aligned}\beta = {} & \frac{2\rho\sqrt{P}\{(\chi^I - \tilde{\chi}^I)\eta^Q + (\chi^Q - \tilde{\chi}^Q)\eta^I\}}{\sigma_{\eta^I}\sigma_{\eta^Q}} - \frac{2\sqrt{P}(\chi^I - \tilde{\chi}^I)\eta^I}{\sigma_{\eta^I}^2} \\ & - \frac{2\sqrt{P}(\chi^Q - \tilde{\chi}^Q)\eta^Q}{\sigma_{\eta^Q}^2} - \frac{E(\chi^I - \tilde{\chi}^I)^2}{\sigma_{\eta^I}^2} - \frac{E(\chi^Q - \tilde{\chi}^Q)^2}{\sigma_{\eta^Q}^2} \\ & + \frac{2\rho E\{(\chi^I - \tilde{\chi}^I)(\chi^Q - \tilde{\chi}^Q)\}}{\sigma_{\eta^I}\sigma_{\eta^Q}}.\end{aligned} \tag{19}$$

Without loss of generality β, conditioned on χ, is a Gaussian RV with the following mean and variance values

$$\mu_\beta = \frac{E\|\chi^I - \tilde{\chi}^I\|^2}{\sigma_{\eta^I}^2} + \frac{E\|\chi^Q - \tilde{\chi}^Q\|^2}{\sigma_{\eta^Q}^2} - \frac{2\rho E(\chi^I - \tilde{\chi}^I)(\chi^Q - \tilde{\chi}^Q)}{\sigma_{\eta^I}\sigma_{\eta^Q}}, \tag{20}$$

$$\sigma_\beta^2 = 4E(1-\rho^2)\left\{\frac{E\|\chi^I - \tilde{\chi}^I\|^2}{\sigma_{\eta^I}^2} + \frac{E\|\chi^Q - \tilde{\chi}^Q\|^2}{\sigma_{\eta^Q}^2} - \frac{2\rho(\chi^I - \tilde{\chi}^I)(\chi^Q - \tilde{\chi}^Q)}{\sigma_{\eta^I}\sigma_{\eta^Q}}\right\}. \tag{21}$$

Using (18) and (20), the conditional PEP (CPEP) can be written as in (22) on the top of the page, where $Q(x)$ denotes the Q-function defined as $Q(x) = 1/2\pi\int_x^\infty \exp(-u^2/2)du$.

$$\mathrm{CPEP}_{\mathrm{opt}} = Q\left(\sqrt{\frac{P}{4(1-\rho^2)}\left[\frac{\|\chi^I - \tilde{\chi}^I\|^2}{\sigma_{\eta^I}^2} + \frac{\|\chi^Q - \tilde{\chi}^Q\|^2}{\sigma_{\eta^Q}^2} - \frac{2\rho(\chi^I - \tilde{\chi}^I)(\chi^Q - \tilde{\chi}^Q)}{\sigma_{\eta^I}\sigma_{\eta^Q}}\right]}\right) = Q\left(\sqrt{\frac{PY}{2(1-\rho^2)N0}}\right), \tag{22}$$

3.1.2. Traditional ML Detector. Note that the improper behavior of the noise is not considered for the traditional ML detector. Thus, assuming x is transmitted, the PEP of deciding in favor of $\tilde{x}$ is given from the classical ML detector expression in (17) as

$$\begin{aligned}\mathrm{PEP}_{\mathrm{tra}} &= \mathrm{P}_r\left\{\left\|y^{IQ} - \sqrt{P}\chi\right\|^2 > \left\|y^{IQ} - \sqrt{P}\tilde{\chi}\right\|^2\right\} \\ &= \Pr\left\{D > E\|\chi - \tilde{\chi}\|^2\right\},\end{aligned} \tag{23}$$

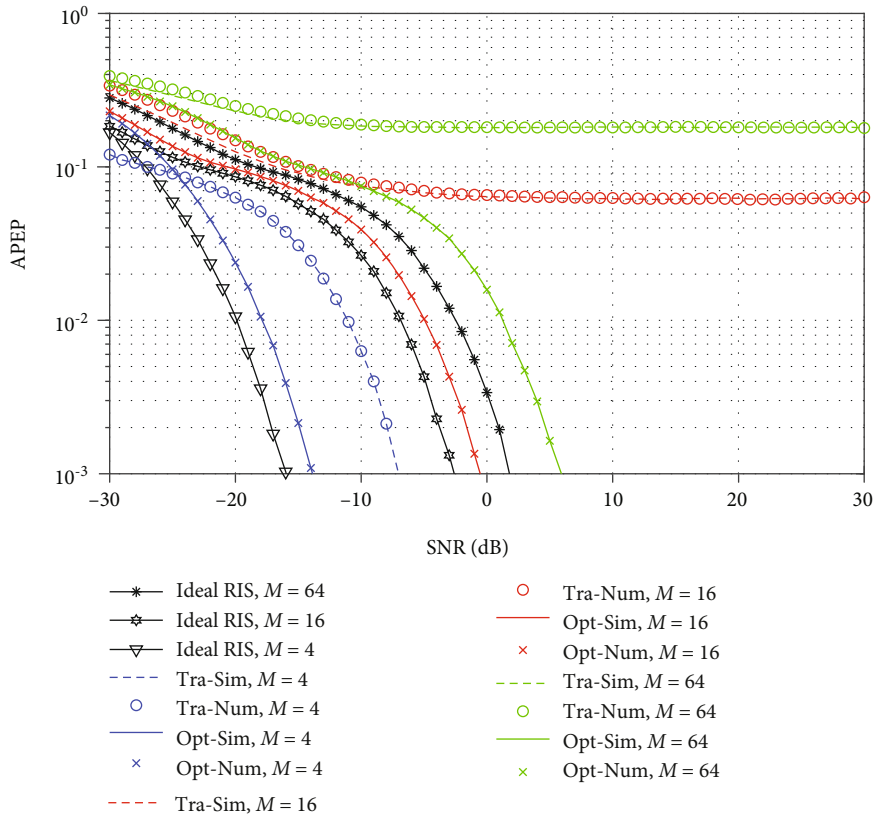

Figure 10: RIS APEP of optimal and traditional ML detector in the presence of joint Tx and Rx IQI with $\varepsilon_t = \varepsilon_r = 3$dB, $\phi_t = \phi_r = 10^\circ$, and $N = 32$ using different modulation order.

where $D = -2R\{\sqrt{P}(\chi - \tilde{\chi})\eta^*\}$ which has zero mean and $\sigma_D^2 = 4P(\chi^I - \tilde{\chi}^I)^2\sigma_{\eta^I}^2 + 4P(\chi^Q - \tilde{\chi}^Q)^2\sigma_{\eta^Q}^2 + 8\rho\sigma_{\eta^I}\sigma_{\eta^Q}P(\chi^I - \tilde{\chi}^I)(\chi^Q - \tilde{\chi}^Q)$ as variance. Hence, the CPEP using Q function is presented in (24).

$$\mathrm{CPEP}_{\mathrm{tra}} = Q\left(\sqrt{\frac{P(\chi^I - \tilde{\chi}^I)^4}{4(\chi^I - \tilde{\chi}^I)^2\sigma_{\eta^I}^2 + 4(\chi^Q - \tilde{\chi}^Q)^2\sigma_{\eta^Q}^2 + 8\rho\sigma_{\eta^I}\sigma_{\eta^Q}(\chi^I - \tilde{\chi}^I)(\chi^Q - \tilde{\chi}^Q)}}\right). \tag{24}$$

3.2. Average Error Probability

3.2.1. Optimal ML Detector. To derive the average PEP (APEP), (22) should be averaged over the PDF of Y which can be depicted as:

$$\mathrm{APEP}_{\mathrm{opt}} = \int_0^\infty Q\left(\sqrt{\frac{PY}{4(1-\rho^2)}}\right) f_Y(Y)dY. \tag{25}$$

However, note that $Y = \Psi_1^2 + \Psi_2^2 - 2\rho\Psi_1\Psi_2$ where $\Psi_1 = (\chi^I - \tilde{\chi}^I)$ and $\Psi_2 = (\chi^Q - \tilde{\chi}^Q)/\xi_r$. Indeed, Ψ_1 and Ψ_2 depend on real and imaginary parts of S and I given in (6). Thus, based on central limit theorem (CLT) and for large number of reflectors N, Y is considered as a combination of correlated noncentral chi-squared random variables. The determination of the APEP using the Y PDF is very hard. Hence, the APEP is numerically computed by averaging PEP over large number of channel realization.

3.2.2. Traditional ML Detector. Traditional ML detector APEP based on (24) is difficult and even impossible to determinate. However, it will be numerically calculated with the same method used for the optimal ML detector.

4. Numerical Results and Discussions

In this part, the APEP performance of the optimal and traditional ML detector for RIS under IQI based on the proposed analytic scenarios will be presented and proved with simulation results.

First, the determined expression of SIR is evaluated in Figures 2 and 3 for different values, respectively, of gains ε_t,

ε_r and phases ϕ_t, ϕ_r of IQI and IRR = 20 dB. It can be depicted that a considerable SIR value degradation occurs even for small imbalance values which highlight the importance of taking into account the IQI in RIS performance analysis.

Figures 4 and 5 are presented to show the effects of, respectively, amplitudes and phases of Tx and Rx IQI on APEP performance. Indeed, in Figure 4, the APEP is analyzed for fixed amplitudes values $\varepsilon_t = \varepsilon_r = 3$dB and for variable values of phase imbalance $\phi_t = \phi_r = [10^\circ, 15^\circ, 25^\circ]$. Accordingly, the effects of increasing the amplitude imbalance from 1dB to 5dB with fixed phases values $\phi_t = \phi_r = 25^\circ$ is given in Figure 5. It can be depicted that increasing the phases and amplitudes of IQI cause a considerable performance loss. Further, the analytical analysis matches perfectly the simulation results for both ML detectors, which validates the proposed analysis. Additionally, it is observed that the proposed ML detector outperforms the classical ML detector for all IQI values and a considerable gain is achieved by using the optimal detector.

Figure 6 shows APEP simulation results of standard ML and optimal ML under only Tx imbalance for different values of ε_t, ϕ_t with $N = 32$. In such case, $\varepsilon_r = \phi_r = 0^\circ$. It is worth mentioning that the optimal design improves the system performance and decreases the IQI effects. The destructive effects of Tx imbalance degrade the performance of perfect RIS. Actually, comparing the ideal RIS with the optimal ML detector performance, the system degrades about 6 dB when $\varepsilon_t = 5$dB and $\phi_t = 25^\circ$, while the degradation is about 1 dB when $\varepsilon_t = 2$dB and $\phi_t = 15^\circ$ at APEP=10^{-2} .

In Figure 7, the impact of Rx IQI on RIS with perfect Tx IQI parameters ($\varepsilon_t = 0, \phi_t = 0^\circ$) is carried for different ε_r, ϕ_r and fixed $N = 32$. For comparison reasons, the case of ideal IQ is also presented. It can be seen the harmful effects of increasing the IQI values on the system performance. Indeed, a 2 dB performance degradation is shown when $\varepsilon_r = 5$dB and $\phi_r = 25^\circ$ for optimal ML compared to the ideal case at APEP=10^{-2}. It can be noticed that there is a performance gain of the designed ML detector compared with the traditional one.

In order to put in evidence the impact of RIS reflector number, Figure 8 presents the numerical and simulation results of optimal and traditional ML detectors under joint Tx and Rx IQI when the number of reflectors changes among 16, 32, and 64. This figure shows the accuracy of the presented analysis for various reflectors numbers. A remarkable performance gain is achieved by using the optimal ML detector. However, even if we increase the number of reflectors, IQI will harm the system performance. For instance, Figure 8 illustrates that if the system has 16 reflectors, the optimal performance degrades by 12 dB when $\varepsilon_t = \varepsilon_r = 5$dB and $\phi_t = \phi_r = 20^\circ$ compared with the perfect IQ matching system at 10^{-3} APEP. This degradation has less impact when increasing the number of reflectors. Hence, it can be concluded that increasing the SNR or the number of reflectors enhances the system performance.

Figure 9 shows the effects of changing IQI parameters at joint Tx and Rx on optimal and standard ML detector performances. The results are carried for fixed IQI parameters at the Tx and Rx $\varepsilon_t = \varepsilon_r = 5$dB, $\phi_t = \phi_r = 10^\circ$ and for different values such as $\varepsilon_t = 5$dB, $\varepsilon_r = 3$dB and $\phi_t = 20^\circ$, $\phi_r = 10^\circ$ with $N = 32$. It can be depicted that the optimal ML detector under equal Tx and Rx IQI parameters outperforms the optimal ML under different values due to the additional mismatch.

Figure 10 validates the derived expressions of optimal and traditional ML detectors for a variable number of modulation order with fixed RIS-IQI parameters $\varepsilon_t = \varepsilon_r = 3$dB, $\phi_t = \phi_r = 10^\circ$, and $N = 32$. It can be shown that RIS using conventional ML detector with increased modulation order suffers from an error floor in the high SNR region due to the fact of ignoring the noise behavior. Consequently, in the presence of IQI, RIS with a traditional ML detector could not support high order modulation which is not acceptable in practice. A careful study for high data rate RIS-aided communication systems in the presence of IQI is required. However, the designed optimal ML detector prevents the error floor and decreases the IQI impairments.

5. Conclusion

This paper investigates the harmful effects of IQI on RIS-aided communication. Hence, novel analytical expressions of PEP and the APEP for optimal and traditional ML detectors are derived. Consequently, the behavior of the designed detectors is analyzed in function of Tx and Rx IQ parameters to further characterize the effects of IQI. Finally, numerical results are illustrated to prove the efficiency of the proposed analysis. The carried results highlight RIS performance degradation's with the presence of IQI even in high SNR regions and an increased number of reflectors. It was proved for the different carried cases that optimal ML detector performs far better than conventional detection method. However, it is worth noting that an optimal detector presents a significant computational complexity. Hence, studying IQI compensation algorithms with low complexity for RIS systems could be potential future works. Moreover, we intend to analyze the performance of RIS under IQI with the presence and absence of direct links between the source and the destination.

Data Availability

The data that support the findings of this study are available from the corresponding author.

Conflicts of Interest

The authors declare that they have no conflicts of interest.

References

[1] A. Gupta and R. K. Jha, "A survey of 5G network: architecture and emerging technologies," *IEEE Access*, vol. 3, pp. 1206–1232, 2015.

[2] K. David and H. Berndt, "6G vision and requirements: is there any need for beyond 5G?," *IEEE Vehicular Technology Magazine*, vol. 13, no. 3, pp. 72–80, 2018.

[3] C. Huang, A. Zappone, G. C. Alexandropoulos, M. Debbah, and C. Yuen, "Reconfigurable intelligent surfaces for energy

efficiency in wireless communication," *IEEE Transactions on Wireless Communications*, vol. 18, no. 8, pp. 4157–4170, 2019.

[4] E. Basar, M. di Renzo, J. de Rosny, M. Debbah, M. S. Alouini, and R. Zhang, "Wireless communications through reconfigurable intelligent surfaces," *IEEE Access*, vol. 7, pp. 116753–116773, 2019.

[5] M. Di Renzo, M. Debbah, D. T. Phan-Huy et al., "Smart radio environments empowered by reconfigurable AI meta-surfaces: an idea whose time has come," *EURASIP Journal on Wireless Communications and Networking*, vol. 2019, no. 1, Article ID 129, 2019.

[6] Q. Wu and R. Zhang, "Towards smart and reconfigurable environment: intelligent reflecting surface aided wireless network," *IEEE Communications Magazine*, vol. 58, no. 1, pp. 106–112, 2020.

[7] S. Hu, F. Rusek, and O. Edfors, "Beyond massive MIMO: the potential of data transmission with large intelligent surfaces," *IEEE Transactions on Signal Processing*, vol. 66, no. 10, pp. 2746–2758, 2018.

[8] E. Bjornson, O. Ozdogan, and E. G. Larsson, "Intelligent reflecting surface versus decode-and-forward: how large surfaces are needed to beat relaying?," *IEEE Wireless Communications Letters*, vol. 9, no. 2, pp. 244–248, 2019.

[9] A. N. Parks, A. Liu, S. Gollakota, and J. R. Smith, "Turbocharging ambient backscatter communication," *ACM SIGCOMM Computer Communication Review*, vol. 44, no. 4, pp. 619–630, 2015.

[10] T. S. Rappaport, G. R. MacCartney, M. K. Samimi, and S. Sun, "Wideband millimeter-wave propagation measurements and channel models for future wireless communication system design," *IEEE Transactions on Communications*, vol. 63, no. 9, pp. 3029–3056, 2015.

[11] J. G. Andrews, X. Zhang, G. D. Durgin, and A. K. Gupta, "Are we approaching the fundamental limits of wireless network densification?," *IEEE Communications Magazine*, vol. 54, no. 10, pp. 184–190, 2016.

[12] C. Liaskos, S. Nie, A. Tsioliaridou, A. Pitsillides, S. Ioannidis, and I. Akyildiz, "A new wireless communication paradigm through software controlled metasurfaces," *IEEE Communications Magazine*, vol. 56, no. 9, pp. 162–169, 2018.

[13] A. C. Tasolamprou, A. Pitilakis, S. Abadal et al., "Exploration of intercell wireless millimeter-wave communication in the landscape of intelligent metasurfaces," *IEEE Access*, vol. 7, pp. 122931–122948, 2019.

[14] M. A. ElMossallamy, H. Zhang, L. Song, K. G. Seddik, Z. Han, and G. Y. Li, "Reconfigurable intelligent surfaces for wireless communications: principles, challenges, and opportunities," *IEEE Transactions on Cognitive Communications and Networking*, vol. 6, no. 3, pp. 990–1002, 2020.

[15] L. Dai, B. Wang, M. Wang et al., "Reconfigurable intelligent surface-based wireless communications: antenna design, prototyping, and experimental results," *IEEE Access*, vol. 8, pp. 45913–45923, 2020.

[16] X. Yuan, Y. J. Zhang, Y. Shi, W. Yan, and H. Liu, "Reconfigurable-intelligent-surface empowered 6G wireless communications: challenges and opportunities," 2020, arXiv preprint.

[17] J. V. Alegría and F. Rusek, "Achievable rate with correlated hardware impairments in large intelligent surfaces," in *2019 IEEE 8th International Workshop on Computational Advances in Multi-Sensor Adaptive Processing (CAMSAP)*, pp. 559–563, Le gosier, Guadeloupe, December 2019.

[18] M. Jung, W. Saad, Y. Jang, G. Kong, and S. Choi, "Reliability analysis of large intelligent surfaces (LISs): rate distribution and outage probability," *IEEE Wireless Communications Letters*, vol. 8, no. 6, pp. 1662–1666, 2019.

[19] M. Jung, W. Saad, Y. Jang, G. Kong, and S. Choi, "Performance analysis of large intelligence surfaces (LISs): asymptotic data rate and channel hardening effects," 2018, https://arxiv.org/abs/1810.05667.

[20] S. Gong, X. Lu, D. T. Hoang et al., "Toward smart wireless communications via intelligent reflecting surfaces: a contemporary survey," *IEEE Communications Surveys and Tutorials*, vol. 22, no. 4, pp. 2283–2314.

[21] T. Schenk, *RF Imperfections in High-Rate Wireless Systems: Impact and Digital Compensation*, Springer Publishing Company, Incorporated, 1st edition, 2008.

[22] J. Li, M. Matthaiou, and T. Svensson, "I/Q imbalance in AF dual-hop relaying: performance analysis in Nakagami-m fading," *IEEE Transactions on Communications*, vol. 62, no. 3, pp. 836–847, 2014.

[23] A. E. Canbilen, M. M. Alsmadi, E. Basar, S. S. Ikki, S. S. Gultekin, and I. Develi, "Spatial modulation in the presence of I/Q imbalance: optimal detector and performance analysis," *IEEE Communications Letters*, vol. 22, no. 8, pp. 1572–1575, 2018.

[24] A. E. Canbilen, S. S. Ikki, E. Basar, S. S. Gultekin, and I. Develi, "Impact of I/Q imbalance on amplify-and-forward relaying: optimal detector design and error performance," *IEEE Transactions on Communications*, vol. 67, no. 5, pp. 3154–3166, 2019.

[25] M. M. Alsmadi, A. E. Canbilen, N. Abu Ali, S. S. Ikki, and E. Basar, "Cognitive networks in the presence of I/Q imbalance and imperfect CSI: receiver design and performance analysis," *IEEE Access*, vol. 7, pp. 49765–49777, 2019.

[26] S. Li, L. Yang, D. B. . Costa, M. D. Renzo, and M. S. Alouini, "On the performance of RIS-assisted dual-hop mixed RF-UWOC systems," *IEEE Transactions on Cognitive Communications and Networking*, vol. 7, no. 2, pp. 340–353, 2021.

[27] F. A. P. de Figueiredo, M. S. P. Facina, R. C. Ferreira et al., "Large intelligent surfaces with discrete set of phase-shifts communicating through double-Rayleigh fading channels," *IEEE Access*, vol. 9, pp. 20768–20787, 2021.

[28] I. Trigui, E. K. Agbogla, M. Benjillali, W. Ajib, and W. P. Zhu, "Bit error rate analysis for reconfigurable intelligent surfaces with phase errors," *IEEE Communications Letters*, vol. 25, no. 7, pp. 2176–2180, 2021.

[29] Y. Zou, M. Valkama, and M. Renfors, "Digital compensation of I/Q imbalance effects in space-time coded transmit diversity systems," *IEEE Transactions on Signal Processing*, vol. 56, no. 6, pp. 2496–2508, 2008.

[30] T. Schenk, *IQ imbalance. RF Imperfections in High-rate Wireless Systems: Impact and Digital Compensation*Springer, Dordrecht.

[31] B. Selim, S. Muhaidat, P. C. Sofotasios et al., "Performance analysis of non-orthogonal multiple access under I/Q imbalance," *IEEE Access*, vol. 6, pp. 18453–18468, 2018.

[32] B. Razavi, *RF Microelectronics*, Prentice-Hall, Inc., Upper Saddle River, NJ, USA, 1998.

[33] A. A. Boulogeorgos, V. M. Kapinas, R. Schober, and G. K. Karagiannidis, "I/Q-imbalance self-interference coordination," *IEEE Transactions on Wireless Communications*, vol. 15, no. 6, pp. 4157–4170, 2016.

[34] A.-A. A. Boulogeorgos, P. C. Sofotasios, B. Selim, S. Muhaidat, G. K. Karagiannidis, and M. Valkama, "Effects of RF impairments in communications over cascaded fading channels," *IEEE Transactions on Vehicular Technology*, vol. 65, no. 11, pp. 8878–8894, 2016.